International Journal of Design & Nature and Ecodynamics
Vol. 20, No. 8, August, 2025, pp. 1745-1758
Journal homepage: http://iieta.org/journals/ijdne

Nano-Silica Oxide Modified Porcelanite for Enhanced Adsorption of Levofloxacin from Aqueous Solution

Zainab Khalil*, Khalid Khazzal Hummadi

Department of Environmental Engineering, College of Engineering, University of Baghdad, Baghdad 10071, Iraq

Corresponding Author Email: dr.khalid.Hummadi@coeng.uobaghdad.edu.iq

https://doi.org/10.18280/ijdne.200806

Received: 19 July 2025
Revised: 20 August 2025
Accepted: 25 August 2025
Available online: 31 August 2025

Keywords:
adsorption, levofloxacin, nano silica, porcelanite

ABSTRACT

This study examines the effectiveness of natural Iraqi porcelanite and silica nanoparticle-coated porcelanite (NanoSiO$_2$/porcelanite) in removing levofloxacin (LEVOX) from water. FTIR, XRD, and SEM were used to characterize the adsorbent before and after the adsorption process. Different conditions were investigated, including contact time, pH, initial concentration, dosages, particle size, and temperature. The results showed that the functional groups, such as carbonyl and hydroxyl, on the surface of NanoSiO$_2$/porcelanite and porcelanite played a key role in the adsorption and retention of antibiotic molecules. The best adsorption conditions for a 10 mg/L LEVOX solution were 0.15 g/50 mL for porcelanite and 0.08 g/50 mL for NanoSiO$_2$/porcelanite, a particle size of 424 µm, a shaking speed of 200 rpm, with a pH of around 6 and 6.5 with maximum adsorption percentage of 74 and 91 for porcelanite and NanoSiO$_2$/porcelanite, respectively, and a temperature of 298.15 K. The experimental adsorption data for LEVOX on porcelanite and NanoSiO$_2$/porcelanite fit the pseudo-second order kinetics. In contrast, the isotherm study confirmed that the Langmuir model fits better for porcelanite and NanoSiO$_2$/porcelanite. The maximum adsorption capacity was 52.322 and 130 mg/g for porcelanite and NanoSiO$_2$/porcelanite, respectively. The thermodynamic analysis reveals that the negative ΔHo value illustrates the exothermic nature of the adsorption process, and the adsorption of LEVOX from aqueous solution was a chemisorption process for both porcelanite and NanoSiO$_2$/porcelanite. Surface modification of porcelanite using silica nanoparticles resulted in a marked enhancement of its performance characteristics, underscoring the effectiveness of Nano-SiO$_2$ treatment. The observed improvements position modified forms of porcelanite as cost-effective and promising adsorbents for the remediation of pharmaceutical contaminants from aqueous systems.

1. INTRODUCTION

Pharmaceutical pollution, especially from antibiotics such as LEVOX, is a significant worldwide environmental issue due to pollutants' persistence, ecological toxicity, and contribution to the acceleration of antimicrobial resistance. Conventional wastewater treatment facilities frequently do not effectively eliminate these contaminants, highlighting the need to create innovative, efficient, cost-effective adsorbents [1]. Many adsorbents, such as montmorillonite, activated sludge-derived activated carbon, kaolinite, modified coal fly ash, Titanium oxide aggregates, and biochar, were used to remove fluoroquinolone antibiotics, which have their own drawbacks and advantages [2-10]. Silica-based materials have been utilized to develop novel composites with exceptional contaminant adsorption capabilities for removing organic pollutants from aqueous solution [11]. Prior studies reveal that the naturally abundant siliceous porcelanite material is a promising and low-cost adsorbent for dyes and heavy metals. However, its effectiveness in treating pharmaceutical pollutants suffers from the relatively small surface and limited number of active sites [12, 13]. Surface modification using nanomaterials, especially Nano-silica (NanoSiO), is increasingly conducted to overcome these issues. The Nano-silica offers a high surface area, abundant surface hydroxyl groups, and strong reactivity. These features enhance desorption via π–π stacking, electrostatic interactions, and hydrogen bonding. It has been confirmed that nano-silica composites are effective in removing a diverse range of organic contaminants, including the antibiotics Ciprofloxacin [14, 15] and Norfloxacin [16]. Although previous research has investigated various natural and engineered materials for removing pharmaceutical pollutants from water, the use of nano-silica-coated porcelanite specifically for LEVOX adsorption remains largely unaddressed in the literature. This study introduces a novel adsorbent by functionalizing naturally occurring porcelanite with silica nanoparticles, thereby enhancing its surface area and the availability of active binding sites. The unique combination of these materials has not been previously explored for LEVOX removal, distinguishing this work from existing studies. However, the removal of levofloxacin, a widely used fluoroquinolone antibiotic, using low-cost, sustainable adsorbents is still insufficiently studied. This research develops a novel hybrid

adsorbent based on Nano-SiO_2-porcelanite to improve LEVOX removal. The specific objectives are to:

1. Characterize the structural, morphological, and surface chemical properties of both raw porcelainite and the nano-SiO_2-coated variant using analytical techniques including FTIR, BET, SEM, and XRD.
2. Assess the adsorption performance of raw versus modified porcelainite under operational parameters such as solution pH, initial levofloxacin concentration, contact time, and adsorbent dosage.
3. Model the adsorption behavior via isotherm and kinetic analyses, comparing the uptake capacity and rate between materials.
4. Elucidate the role of surface functional groups—especially silanol and aluminol—and their interaction mechanisms with levofloxacin's reactive sites in both raw and coated forms.
5. Assess the practical feasibility and environmental promise of the hybrid nano-SiO_2-coated porcelainite in converting into a scalable adsorbent for pharmaceutical wastewater remediation.

2. MATERIALS AND METHODS

2.1 Chemical

A chemical was supplied by the Samarra, Iraq-based General Company for the Drugs Industry for the (LEVOX) ($C_{18}H_{20}FN_3O_4$)—formula with a molecular weight of 361.4 g/mole, as shown in Figure 1. The ethanol (C_2H_6O) with 99.9% purity and the ammonia solution (NH_3) with 99.9% purity were supplied by LOBA CHEMIE, an Indian company. Glentham Life Sciences provided Tetraethoxysilane (TEOS, $C_8H_{20}O_4Si$) in a volume of 10 mL with a purity of 99%, and silica gel (3-5 mm) was provided by Fisher Scientific. Acetic Acid Glacial (CH_3CO_2H): Alpha Chemika, an Indian company, produces hydrochloric acid (HCl) (37% purity). Alpha Chemika, an Indian company, produces sodium hydroxide (NaOH) with 97% purity, while LOBA CHEMIE, also an Indian company, supplies acetone (CH_3COCH_3) with 99.5% purity. ACS Chemical is an Indian company. deionized water was used (GFL, Type 2001/4, Germany) to make all of the solutions.

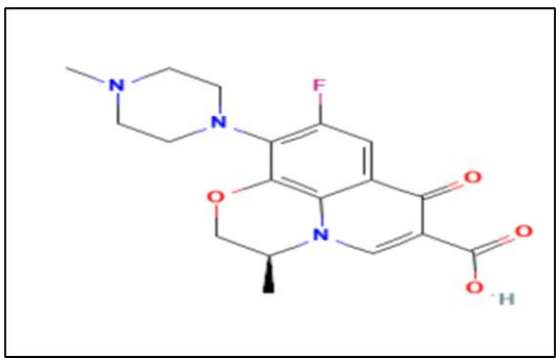

Figure 1. LEVOX chemical structure [17]

2.2 Adsorbents

In this study, we used Porcelanite as a natural, low-cost adsorbent. It was obtained from the Geological Survey Department at the Iraqi Ministry of Industry. The rock was manually crushed into tiny pieces, then rinsed thoroughly with distilled water to remove dirt or loose particles. After washing, the pieces were left to dry completely at room temperature. Once dried, we used a sieve to separate particles, focusing on our experiments' 425 µm size range.

2.3 Preparation of LEVOX stock solution

In a LEVOX, the chosen adsorbate is a common antibiotic often found in pharmaceutical effluent. The chemical formula for the substance is $C_{18}H_{20}FN_3O_4$, and its molecular weight is 361.37 g/mol. It takes ultraviolet-visible (UV-Vis) light at about 330 nm. The LEVOX used in this study had a purity of at least 99% and was bought from local pharmacies. This is similar to how unwanted or expired drugs are often thrown away in the real world. We mixed some LEVOX powder with 1 liter of distilled water to make the stock solutions. We made this answer as needed during the studies to ensure its correctness. We carefully altered the pH of all the solutions by slowly adding either 1 M NaOH or HCl, depending on the test's needs.

2.4 Preparing nanomaterial silica and synthesis of NanoSiO₂/porcelanite

Using a metric converter, Tetraethoxysilane (TEOS) was combined with ethyl alcohol solvent in a 1:1 volume ratio. 1 mL of M1 dropwise hydrochloric acid (HCl) was then added to start and accelerate the process. To accomplish full hydrolysis, the solution was agitated for two hours at 400 rpm. The liquid was chilled to prevent early gel formation since acid catalysis speeds up hydrolysis more than base catalysis. The resulting acid-catalyzed nano-dispersed silica sol was produced after the reaction. Usually, this sol gels in a few days. As seen in Figure 2, the produced gel was thus heated to 250°C for three to four hours in order to create silica nanopowder [18].

Figure 2. Preparation steps of $NanoSiO_2$

As shown in Figure 3, the porcelanite was washed with a 1 M HCl solution. Then, it was washed with distilled water to reach a pH of 7 and then dried at 100°C. Afterwards, in a beaker, dispense an appropriate amount (5 g) of dry porcelanite into an Acetone solution (100 mL) on a stirrer for 10 minutes, and transfer the beaker to an ultrasonic device, then add 0.5 g of $NanoSiO_2$ Nano particles to disperse the SiO_2

Nano particles onto the porcelanite surface for 60 seconds. The mixture was transferred into an autoclave reactor. After 24 hours, the mixture was filtered, and the NanoSiO$_2$/porcelanite was dried at 100°C for 24 hours [19].

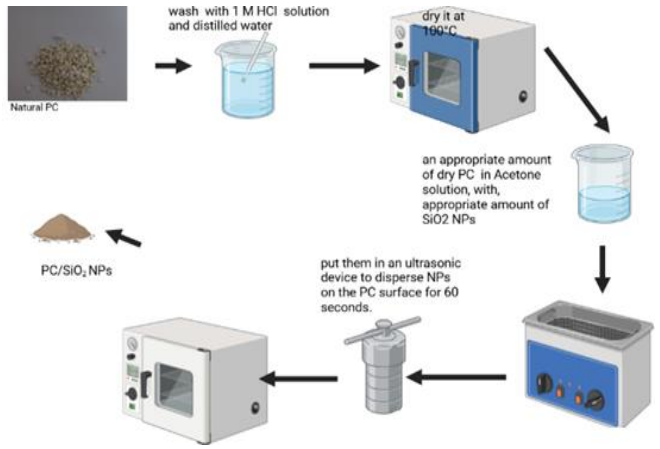

Figure 3. Synthesis steps of NanoSiO$_2$/porcelanite

2.5 Determination of the pHpzc

There are numerous methods for measuring pHpzc, one of which is the solid addition method. Different 250 mL conical flasks filled with 100 mL of 0.1 mol/L sodium chloride solution were prepared, and each flask had a different pH adjusted between 2 and 11 with HCl or NaOH. Then 1 g of porcelanite and porcelanite/SiO$_2$ Nano particles were added to each conical flask and mixed after 24 hours. We calculated the pH of the initial and final solutions and recorded their differences. The point of zero charges is 7.34. The nanoparticle surface of the porcelanite/SiO$_2$ exhibits a net negative charge at pH > 7.34, while at pH < 7.34, the surface charge becomes positive [20].

3. RESULTS AND DISCUSSION

3.1 Characterization of adsorbent

Several analytical methods, including as Fourier Transform Infrared Spectroscopy (FTIR), X-ray Diffraction (XRD), and Scanning Image Analysis, are commonly used to characterise the samples, including X-ray Diffraction (XRD), Fourier Transform Infrared Spectroscopy (FTIR), Scanning Electron Microscopy (SEM), and Energy Dispersive X-ray Spectroscopy (EDS). The XRD analysis revealed the mineralogical composition of the crystalline phase. The FTIR is employed to characterize the samples' functional groups and chemical bonding. While the surface morphology and textural features are examined using SEM, with EDS analysis enabling localized elemental microanalysis. The XRF spectroscopy provided the quantitative values of the elemental composition data. Additionally, BET surface area analysis quantified key parameters such as specific pore volume, porosity, and surface area, which are crucial factors prevailing in the adsorption behavior and catalytic reactivity. Modifications to porcelanite samples, including thermal activation and chemical treatments, are expected to change their physicochemical features. The comparison between ordinary and modified samples enables assessment of the efficacy in enhancing material features for targeted applications such as catalytic substrates, wastewater remediation, and construction materials.

The study proposes a new hybrid approach that uses multiple techniques for robust material characterization. The proposed approach aims to understand the transformation and optimization of natural materials and optimize them for real-world applications.

3.2 Fourier transform infrared spectroscopy analysis

Figure 4 presents the FTIR analysis of the prepared NanoSiO$_2$, where multiple distinct absorption bands are visible. Notably, the peak observed at 420.48 cm^{-1} indicates Si-O bending modes, confirming a signature feature of silicate material [21]. The spectral features at 547.78 cm^{-1} and 574.79 cm^{-1} are characteristic of Si-O-Si bending modes, providing evidence of siloxane linkages [22, 23]. The band at 698.23 cm^{-1}, attributable to Si-OH bending vibrations, implies hydroxyl groups [21]. A band at 802.39 cm^{-1} is assigned to Si-O-Si stretching vibrations, indicative of the silicate network [22]. The band at 954.79 cm^{-1} is related to Si-OH stretching vibrations, confirming the existence of hydroxyl groups [23]. The band at 1095.57 cm^{-1} arises from Si-O-Si stretching vibrations, characteristic of silicate materials [21]. The bands at 1452.40 cm^{-1} (Si-OH stretching vibrations) indicate the surface hydroxyl groups [23]. The Si-OH bending vibrations at band 1537.27 cm^{-1} and adsorbed water bending at band 1647.21 cm^{-1} were observed, confirming moisture exposure during analysis [23]. C-H stretching vibrations observed at bands 2916.37 cm^{-1} suggest possible contamination or organic residue [23]. Finally, the O-H stretching band observed at band 3423.65 cm^{-1} verified the surface hydroxyl groups [22]. The FTIR analysis illustrated in Figure 4 provides detailed insight into the prepared SiO$_2$ sample, revealing (i) silicate linkages, (ii) hydroxyl groups on the surface, and (iii) possible organic contamination.

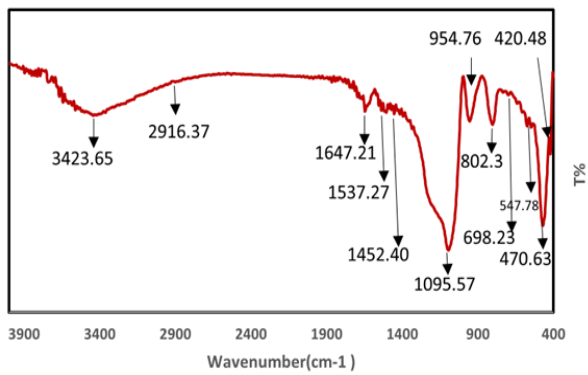

Figure 4. The FTIR analysis of the prepared NanoSiO$_2$

The FTIR analysis of porcelanite (Figure 5) revealed characteristic absorption bands associated with key molecular vibrations including (i) Si-O stretching indicative of silicon-oxygen (472.5 cm^{-1}), (ii) C-C stretching, confirming the existence of alkenes (650.01 cm^{-1}), (iii) C-H bending indicative of aromatic compounds and alkanes (729.09 cm^{-1}), (iv) C-N stretch common in amines and amides (792.74 cm^{-1}), (v) C-Cl stretching seen in chlorinated compounds (879.54 cm^{-1}), C-O stretch suggesting the presence of ethers, alcohols, and esters (1097.50 cm^{-1}), (vi) C-H bending typically seen in methylene groups and alkanes (1423.47 cm^{-1}), (vii) the

complex bands around 1637.56 cm^{-1} (possibly found in C=C, C=O conjugated, or N-H bend), (viii) C=O stretching confirming the carboxylic acids, esters, or aldehydes (1751.36 cm^{-1}), (ix) C-H stretching of alkanes (2947.23 cm^{-1}) and C-H stretching seen in aromatic compounds and alkenes (3024.38 cm^{-1}), (ix) O-H stretching common with phenols and alcohols and N-H stretching in amides and amines (3417.86 cm^{-1}), (x) , and (xi) O-H stretching of hydroxyl groups (3549.02 cm^{-1}) . upon coating porcelanite with Nano-SiO_2, additional bands and shifts in existing bands were observed: 474.49 cm^{-1} (Si-O stretching indicating enhanced silicon-oxygen bonding), 650.01 cm^{-1} (C-C stretching), 729.09 cm^{-1} (C-H bending), 794.67 cm^{-1} (C-N stretching), 881.47 cm^{-1} (C-Cl stretching), 991.41 cm^{-1} (new C-O stretching band in ethers or alcohols), 1087.85 cm^{-1} (shift in C-O stretching), 1453.33 cm^{-1} (new C-H bending band), 1631.78 cm^{-1} (shift in C=C or C=O stretching in conjugated systems, or N-H bending), 1712.79 cm^{-1} (shift in C=O stretching), 2995.45 cm^{-1} (shift in C-H stretching), 3375.43 cm^{-1} (shift in O-H stretching in alcohols/phenols or N-H stretching in amines/amides), and 3560.00 cm^{-1} (shift in O-H stretching in hydroxyl groups). This comparison reveals new absorption bands and shifts in existing ones due to the Nano-SiO_2 coating, suggesting interactions between the Nano-coating and the original matrix. These changes enhance the material's structural complexity and may influence its properties and performance [5].

FTIR analysis revealed notable changes in surface functional groups following silica modification. The appearance and intensification of Si–O–Si and Si–OH stretching vibrations in the NanoSiO_2/porcelanite spectrum indicate the successful grafting of silanol groups onto the surface. These functional groups are known to enhance adsorptive interactions through hydrogen bonding and electrostatic attractions, particularly with polar pharmaceutical molecules such as levofloxacin, which contains carboxyl, hydroxyl, and amine functionalities. Moreover, the broadening of the O–H stretching region suggests an increase in surface hydroxylation, which contributes to improved hydrophilicity and facilitates greater interaction with aqueous-phase contaminants.

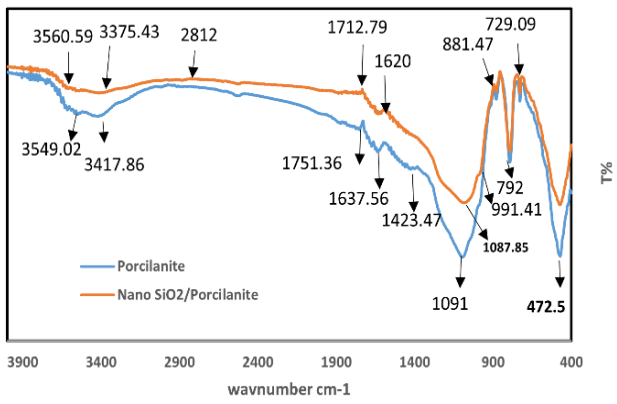

Figure 5. The FTIR analysis of porcelanite and NanoSiO_2/porcelanite

3.3 Scanning electron microscopy analysis

The SEM analysis of Iraqi porcelanite revealed significant microstructural features such as porosity, particle shape, and morphology. Figure 6 shows the EDS and SEM data for the base porcelanite and the Nano-SiO_2-coated version. As seen in Figure 6(A), the particles exhibit irregular to angular shapes, representing the fresh mineral surfaces and minimum mechanical weathering [24]. The Iraqi porcelanite is characterized by a uniform distribution of micro- and mesopores within the matrix. This bimodal porosity enhances the adsorption capacity and surface area, making the material well-suited for industrial and environmental applications. The material morphology also shows a complex featuring tightly packed grains with intergranular voids, resulting in a rough surface texture. This texture enhances the effective surface area, improving chemical reactivity and adsorption capacity [25]. These microstructural properties highlight the suitability of Iraqi porcelanite for various practical applications. After dispersion of nano-SiO_2, SEM analysis of Iraqi porcelanite, shown in Figure 6(B), reveals significant changes that improve the porosity of porcelanite and surface roughness due to uniform particle distribution. The resulting enlargement of the micro- and mesopores increases the surface area and enhances the adsorption effect [26]. Additionally, Nano-SiO_2 increases the complexity of the material morphology by filling intergranular voids, forming a further interconnected pore network. These microstructural changes improve the suitability of Iraqi porcelanite for catalysis applications and environmental remediation. Figure 7 displays the results of SEM and EDS of NanoSiO_2/porcelanite after adsorption of LEVOX. The observed partial pore filling by LEVOX confirms the effectiveness of adsorption efficacy, suggesting that the composite's augmented surface area and porosity facilitate this mechanism, which optimizes its use in environmental and pharmaceutical contexts [5, 26]. These results confirm the potential of NanoSiO_2/porcelanite as an efficient adsorbent for removing pharmaceutical contaminants.

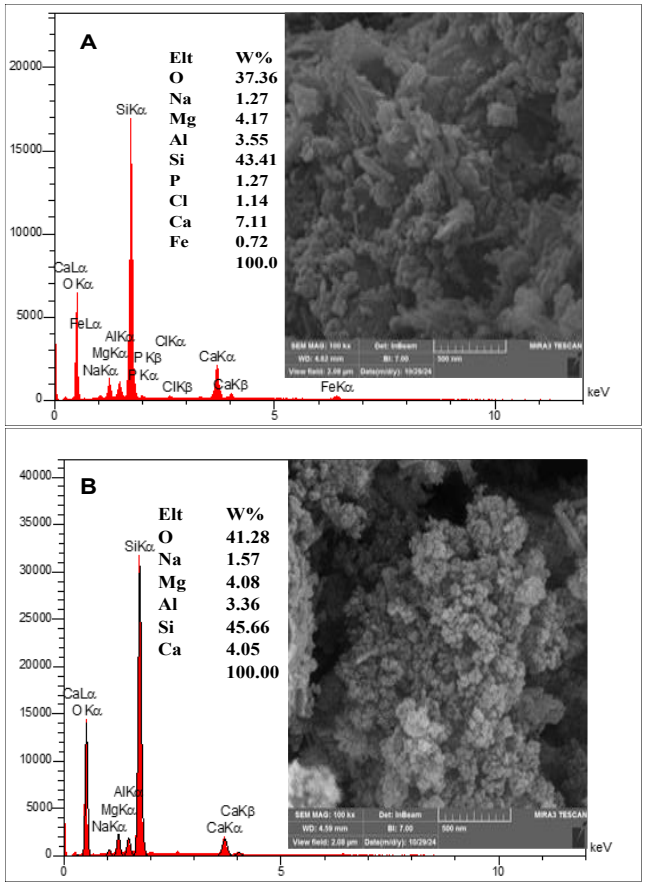

Figure 6. The SEM and EDS data (A) porcelanite and (B) NanoSiO_2/porcelanite

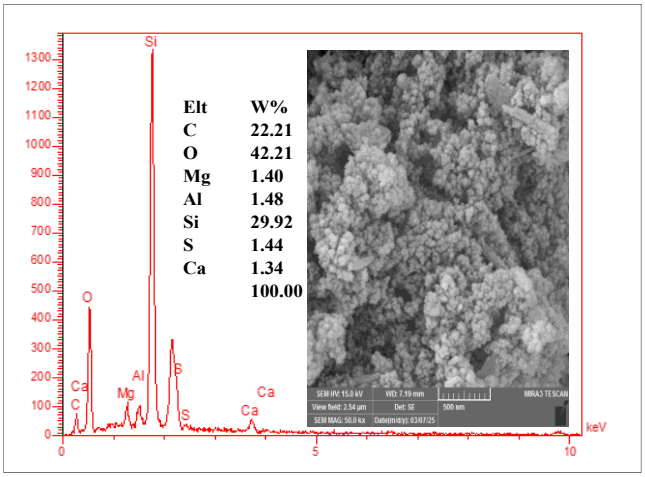

Figure 7. The SEM and EDS data of porcelanite and NanoSiO$_2$/porcelanite after the adsorption of LEVOX

3.4 X-ray diffraction analysis

Figure 8 illustrates the X-ray Diffraction (XRD) of the prepared NanoSiO$_2$. The XRD peaks observed for NanoSiO$_2$ at angles of 20.075°, 33.025°, 37.425°, 45.925°, 61.475°, and a sharp peak at 67.075°, which likely corresponds to the (100), (101), (102), (110), (103), and (112) planes [27], respectively, suggest that the SiO$_2$ nanoparticles have a crystalline structure. These peaks correspond to the typical file from the Joint Committee on Powder Diffraction Standards (JCPDS) number PDF 01-0706. These peaks are associated with specific planes within the crystal lattice of SiO$_2$, indicating a well-organized atomic arrangement. Figure 9(A) indicates the XRD of Iraqi natural porcelanite. The X-ray diffraction (XRD) peaks observed for porcelanite at angles of 21.525°, 21.975°, 26.875°, 31.175°, 36.175°, 41.475°, 51.375°, 60°, and 68.75°, corresponding to the (100), (102), (110), (111), (200), (201), and (210), and the sharp peak at the (100) plane, respectively, indicate a complex crystalline structure. The X-ray diffraction (XRD) peaks observed in Figure 9(B) for SiO$_2$-coated porcelanite at angles indicate the presence of both SiO$_2$ and porcelanite phases. The intensity of peaks that represent the SiO$_2$ is increased. This indicates that the Nano-SiO$_2$ particles dispersed onto the porcelanite reflect the success of preparing the adsorbent. The average particle size of the crystalline for the nanomaterial was identified using the following Debye-Scherrer equation given in Eq. (1) [28].

$$d = \frac{0.89\lambda}{\beta \cos\theta} \quad (1)$$

where, d represents the average size of the crystalline, 0.89 is Scherrer's constant, λ represents the wavelength of the X-ray, β is the FWHM (Full Width at Half Maximum), and θ is the angle of Bragg diffraction. The average crystallite size of the prepared SiO$_2$ was 3.014 and 81 nm for the sample synthesized SiO$_2$ and NanoSiO$_2$/porcelanite, respectively. XRD peaks in Figure 9(C) observed for the material after adsorbing levofloxacin are at angles that indicate the presence of both the original material and LEVOX. The intensity of many peaks is decreased due to the adsorption of LEVOX, which covers the surface of NanoSiO$_2$/porcelanite. These peaks provide valuable insights into the material's crystalline quality and the effects of LEVOX adsorption [29].

Overall, the synergistic effect of increased surface functionality, reduced crystallinity, and improved morphological features explains the significantly enhanced adsorption capacity observed for the NanoSiO$_2$/porcelanite composite. These structural enhancements contribute not only to greater initial uptake but also to improved regeneration performance, highlighting the potential of this material for practical applications in water treatment.

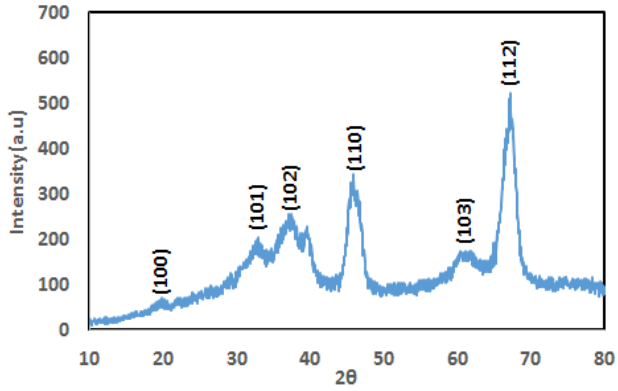

Figure 8. The XRD of the prepared NanoSiO$_2$

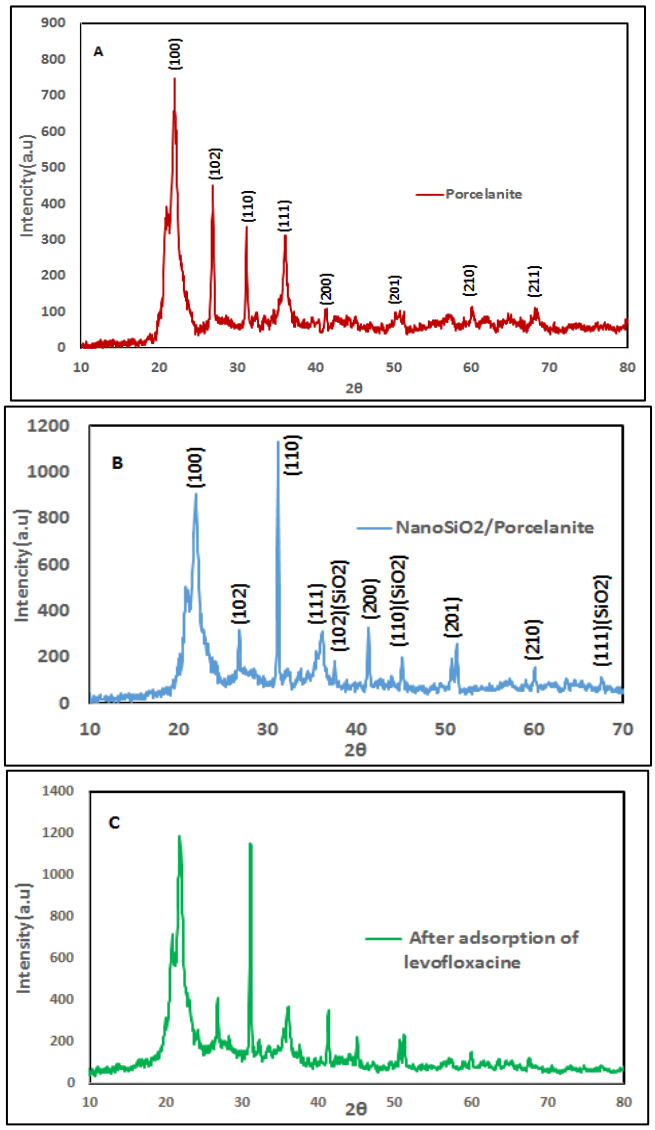

Figure 9. The XRD data of (A) porcelanite, (B) NanoSiO$_2$/porcelanite, and (C) prepared NanoSiO$_2$/porcelanite after adsorption of LEVOX

3.5 The BET analysis

A comprehensive analysis of the surface characteristics demonstrated notable alterations following both nanosilica incorporation and levofloxacin adsorption. The raw porcelanite sample was found to possess a modest specific surface area of 21.166 m^2/g, along with a total pore volume of 0.197 cm^3/g and an average pore diameter of 9.89 nm. After modification with nanoscale SiO_2, a substantial enhancement in surface area was observed, increasing to 66.230 m^2/g. This improvement is attributed to the dispersion of silica nanoparticles across the surface, which likely introduced additional active sites. In contrast, the pore volume and mean pore diameter decreased to 0.098 cm^3/g and 9.370 nm, respectively, suggesting that silica particles partially filled or obstructed existing pores. Subsequent adsorption of levofloxacin led to further reductions in surface area (58.050 m^2/g), pore volume (0.066 cm^3/g), and average pore size (7.989 nm). These observations indicate that levofloxacin molecules were successfully retained within the porous structure, occupying both surface and internal voids of the composite material.

3.6 Adsorption parameters

3.6.1 The effect of pH solution

Understanding the pH-dependent adsorption behaviour is essential for optimizing the LEVOX removal from aqueous solutions in environmental and pharmaceutical applications. The effect of pH on removing LEVOX was studied using natural porcelanite and porcelanite modified with silica nanoparticles ($NanoSiO_2$/porcelanite), under identical conditions, as shown in Figure 10. As the pH increased from 2 to 6-7, the removal efficiency improved, reaching its peak at around pH 6 and 6.5 for porcelanite and $NanoSiO_2$/porcelanite, respectively. After that, the efficiency dropped at higher pH levels. This pattern was seen with both materials, but the $NanoSiO_2$/porcelanite consistently performed better, achieving a maximum removal of about 67%, compared to roughly 43% for the raw material. The improved performance of the modified adsorbent is likely due to its higher surface area and more available adsorption sites. LEVOX is a fluoroquinolone antibiotic with two pKa values: pKa1 = 5.59 (carboxyl group) and pKa2 = 7.94 (amine group). These values determine the ionization states of LEVOX in aqueous solutions: pH less than pKa1, LEVOX is predominantly cationic (positively charged). If pKa1 is between pKa2, LEVOX exists in a zwitterion form. When the pH is greater than pKa2, LEVOX exists in an anionic (negatively charged) form. At lower pH, excess hydrogen ions may compete with LEVOX for these sites. While at higher pH, electrostatic repulsion and changes in the form of the drug could reduce adsorption. The adsorption of levofloxacin onto adsorbents with a pHzpc of approximately 7.34 is maximized at solution pH values near the pKa1 of LEVOX (around 5.59). Beyond this point, as pH increases past the pHzc (7.34) and LEVOX becomes anionic, electrostatic repulsion dominates, leading to a drop in removal.

3.6.2 The effect of dosage

The dosage used is vital in defining contaminant removal efficiency from aqueous systems. For antibiotics like LEVOX, optimizing the adsorbent dose is critical to maximize removal efficiency without unnecessary material use. Typically, increasing adsorbent dosage results in more active sites available for binding, which enhances removal rates at lower doses. However, after a certain threshold, the efficiency gain plateaus, likely due to the saturation of available LEVOX molecules and reduced mass transfer [13, 30].

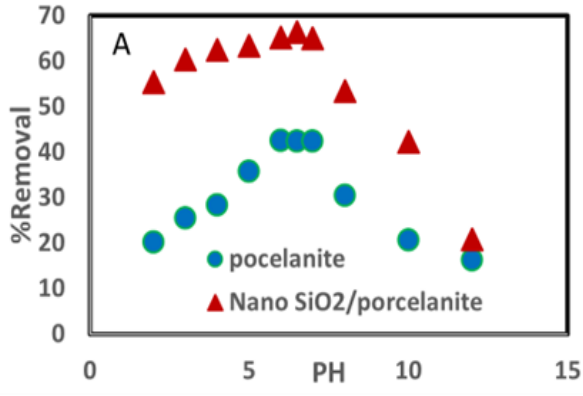

Figure 10. Effect of pH: C0 =50 mg/L, dosage 0.05 g/50 mL, shaking time 2 h, 425 µm particle size, and 200 rpm with different pH of the solution

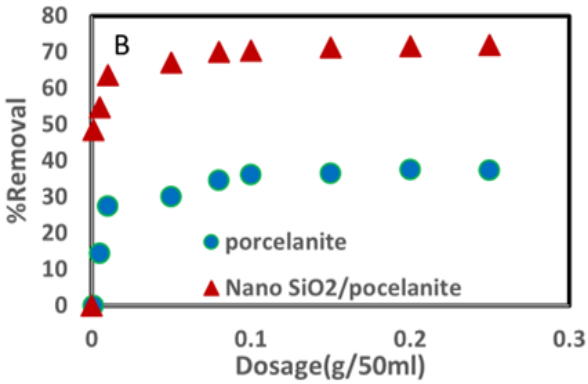

Figure 11. Effect of dosage: C0 = 50 mg/L, pH of solution 6 for porcelanite and 6.5 for $NanoSiO_2$/porcelanite, shaking time 2 h, 425 µm particle size, and 200 rpm with different dosages

This study investigated the dosage effect for natural and Nano-silica-modified porcelanite over 0 to 0.25 g per 50 mL. Tests were conducted at optimized pH values (6.0 for porcelanite and 6.5 for the nano-composite), with a starting LEVOX dosage of 50 mg/L, a 424 µm particle size, a 200 rpm shaking speed, and a 120-minute contact period. Figure 11 shows the effect of the dosage of porcelanite and $NanoSiO_2$/porcelanite for removing LEVOX. A sharp increase in removal efficiency was observed with increasing dosage, especially for the Nano-enhanced material, peaking at around 0.08 g/50 mL and 0.15 g/50 mL for natural porcelanite. Beyond this point, further increases in dosage showed marginal improvements, suggesting the process had reached equilibrium and that excess adsorbent offered limited additional benefit. The Nano-silica-coated adsorbent consistently outperformed unmodified porcelanite, reaching a maximum removal efficiency of ~72%, compared to ~38% for the natural material. This superior performance is attributed to the increased surface area and active functional groups introduced by nano-silica, which enhance adsorption kinetics and interaction with LEVOX molecules [14, 15]. Identifying the appropriate dosage is scientifically important and vital for

economic and environmental sustainability. Overdosing does not linearly improve removal and leads to unnecessary material use. Based on the results, the recommended optimal doses under these conditions are 0.08 g/50 mL for Nano-porcelanite and 0.15 g/50 mL for unmodified porcelanite.

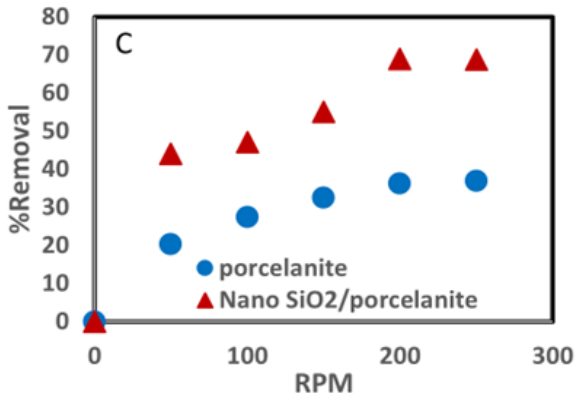

Figure 12. Effect of agitation speed: C0=50 mg/L, pH of solution 6, and 0.08 g/50 mL for NanoSiO_2/porcelanite and PH 6.5 and 0.15 g/50 mL for porcelanite, shaking time 2 h, 425 µm particle size with different rpm

3.6.3 Effect of agitation speed rpm

Agitation is critical in adsorption-based treatment processes, particularly by influencing the mass transfer rate between solutes in the aqueous phase and the surface of the adsorbent. For antibiotics like LEVOX, efficient agitation ensures uniform dispersion of adsorbent particles and maximizes contact opportunities between LEVOX molecules and active sites on the adsorbent surface [31, 32]. This study investigated the effect of agitation speed on the LEVOX removal using two adsorbents: unmodified porcelanite and Nano-silica-modified porcelanite, as stated in Figure 12. Results showed that increasing the agitation speed from static conditions to 200 rpm significantly improved removal efficiency for both materials. However, beyond 200 rpm, no substantial enhancement in performance was observed, indicating that an optimal level of agitation had been reached. This behaviour is attributed to the influence of agitation on the boundary layer thickness surrounding adsorbent particles. A thicker stagnant layer exists at low agitation rates, which hinders the diffusion of LEVOX molecules to the adsorbent surface. As the shaking rate increases, the thickness of the boundary layer decreases, which improves mass transfer and accelerates adsorption. At around 200 revolutions per minute, the boundary layer becomes thinner to optimize mass transfer for adsorption equilibrium [33].

After this point, the scarcity of the active site and intra-particle diffusion determine the adsorption rates, eliminating the need for film diffusion. Mechanical shear due to increased agitation could lead to erosion or desorption, although these did not exist experimentally. Previous studies have described this pattern of metal ion and drug adsorption from aqueous solutions [30, 34]. In both studied materials, the best LEVOX elimination happened at an agitation speed of 200, suggesting that optimization of agitation speed is critical for developing and scaling effective adsorption water treatment systems for antibiotic-contaminated water.

3.6.4 Effect of particle size

Particle size significantly influences solid–liquid adsorption processes by affecting surface area, pore structure, and the diffusion of adsorbate molecules. In pharmaceutical removal, particularly for compounds like LEVOX, smaller particle sizes are generally more effective. This improvement is largely due to the increased surface availability and enhanced mass transfer that smaller particles provide [5, 7]. Smaller particles offer more active sites for adsorption, leading to greater efficiency. From the results of Figure 13, the particle size increases, the available surface area decreases, often resulting in reduced adsorption capacity. This finding highlights the importance of particle size in determining the performance of adsorbents. In this study, both Nano-scale materials and natural porcelanite showed the following trends: Higher LEVOX removal at smaller particle sizes and a consistent decline in removal efficiency as particles became larger, especially when transitioning from Nano to micro-sized fractions. This phenomenon was repeatedly observed across all experimental trials, confirming that surface accessibility plays a crucial role in adsorption performance. The findings suggest that reducing particle size enhances LEVOX removal by increasing the number of exposed surface sites and decreasing the resistance to mass transfer. This behaviour was consistent for both engineered Nano-adsorbents and natural materials, underscoring the critical role of surface area in removing pharmaceutical contaminants from water.

3.6.5 Effect of initial concentration

Figure 14 illustrates that the efficiency of LEVOX removal depends directly on the starting concentration. With a maximum of active sites, high efficiency happens at low concentrations. On the other hand, site saturation happens at higher concentrations, leading to a decrease in removal rates. The experimental data confirm that adsorbents (i.e., Nano-SiO_2 and natural porcelanite) achieve optimal removal at low concentrations and decreasing efficiency as LEVOX concentrations increase. Nano-enhanced SiO_2/porcelanite materials consistently outperformed the unmodified variants, maintaining superior adsorption efficiency across various concentrations. This trend highlights the limitation of traditional adsorbents under high contaminant loads and the enhanced capacity of Nano-structured materials. The superior performance of Nano-SiO_2 composites can be attributed to their greater surface area and higher density of active sites [5, 34], making them particularly effective for treating high-strength pharmaceutical effluents.

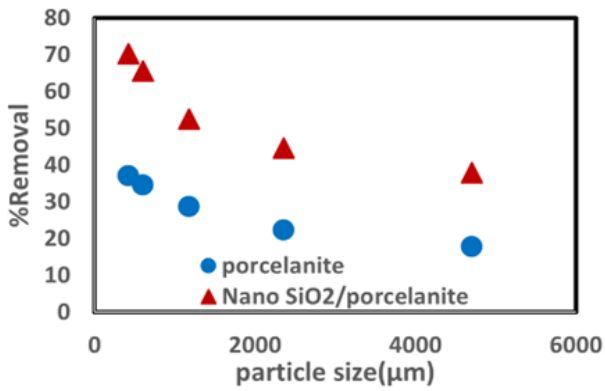

Figure 13. Effect of particle size: C0 = 50 mg/L, pH of solution 6.5 and 0.08 g/50 mL for NanoSiO_2/porcelanite, and pH 6, 0.15 g/50 mL for porcelanite, shaking time 2 h, and 200 rpm with different particle sizes

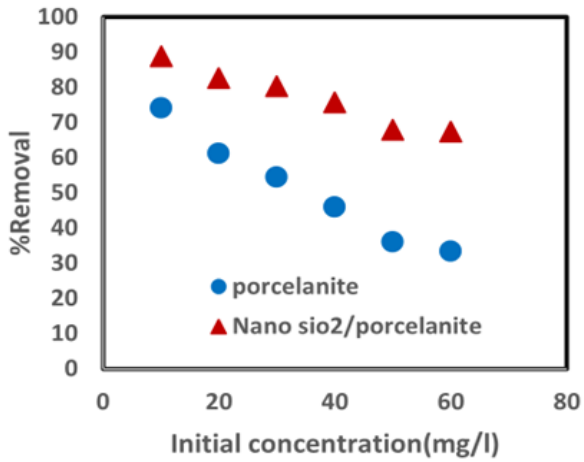

Figure 14. Effect of initial concentration: pH of solution 6.5 and 0.08 g/50 mL for NanoSiO$_2$/porcelanite and pH 6 and 0.15 g/50 mL for porcelanite, shaking time 2 h, and 200 rpm with different initial concentrations

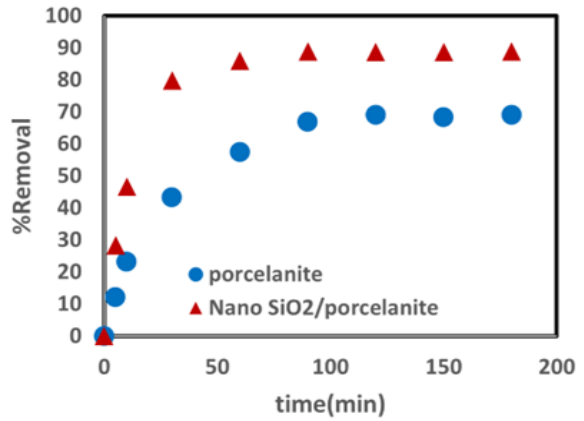

Figure 15. Effect of time: C0 = 10 mg/L, pH of solution 6.5, and 0.08 g/50mL for NanoSiO$_2$/porcelanite, and pH 6.5 and 0.15 g/50 mL for porcelanite, and 200 rpm with different times of shaking

3.6.6 Effect of time

Contact time is vital in adsorption processes, influencing the required time to reach equilibrium. For LEVOX, understanding adsorption kinetics is key to maximizing removal efficiency. In this study, the performance of raw porcelanite and a Nano-SiO$_2$-coated variant was assessed across different contact times to evaluate the time influence of LEVOX. As shown in Figure 15, the adsorption process generally follows three distinct stages: the initial rapid phase (0–30 minutes), characterized by a high adsorption rate due to the abundance of unoccupied active sites. Slower transitional phase (30–120 minutes). As more sites are filled, the adsorption rate decreases due to a lower concentration gradient and increased competition—equilibrium phase (after 120 minutes). A state is reached where the rates of adsorption and desorption balance out. Removal efficiency improved over time and plateaued around the 120-minute mark for both adsorbents. However, the Nano-SiO$_2$-coated material demonstrated quicker adsorption kinetics and higher overall LEVOX uptake. This improved performance is likely due to better diffusion dynamics and greater accessibility to binding sites created by the Nano-coating [5, 35]. These results highlight the advantages of surface-engineered materials, with the Nano-coated adsorbent offering significantly enhanced performance for pharmaceutical removal. The evidence suggests that surface modification can be a valuable strategy for improving adsorption-based water treatment technologies.

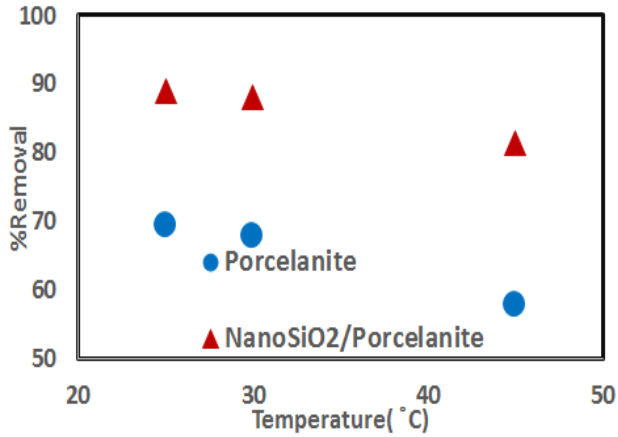

Figure 16. Effect of temperature: C0 = 10 mg/L, pH of solution 6.5 and 0.08 g/ 50mL for NanoSiO$_2$/porcelanite and pH 6 and 0.15 g/ 50mL for porcelanite, 2 h, and 200 rpm with different temperatures

3.6.7 Effect of temperature

Temperature is a key parameter in adsorption studies, as it influences the process's feasibility and the interactions between the adsorbate and the adsorbent. In the case of LEVOX removal, evaluating temperature effects provides insight into whether the adsorption is thermodynamically favorable and whether the process is endothermic or exothermic. The impact of temperature on LEVOX adsorption using natural porcelanite and Nano-SiO$_2$-coated adsorbents is shown in Figure 16. A decline in adsorption efficiency was observed when the temperature increased, suggesting that the process is exothermic. The highest removal efficiency was achieved at around 25°C, likely due to enhanced molecular mobility and diffusion at moderately elevated temperatures. The exothermic nature of the adsorption indicates that the process is more effective at room or lower temperatures, making it suitable for energy-efficient applications [34]. The lack of need for external heating simplifies system design. It reduces operational costs, making this approach practical for treating pharmaceutical wastewater and decentralized or point-of-use water treatment systems.

3.7 Isotherm study of LEVOX adsorption

The adsorption isotherm study illustrates the relation between the quantities of adsorbed material vs. the remaining solution adsorbate concentration. The adsorption of LEVOX onto porcelanite and NanoSiO$_2$/porcelanite was studied in batch operating conditions. The adsorption data were examined using the Langmuir, Freundlich, Redlich-Peterson, and Sips (Eq. (5)) models, which are illustrated in the following Eqs. (2)-(5), respectively, to find the adsorption capacity by applying Eqs. (2)-(4) [5].

$$qe = \frac{qm\ kl\ Ce}{1 + k\ Ce} \tag{2}$$

$$qe = Kf\ C^{1/n} \tag{3}$$

$$qe = \frac{Krp\ Ce}{1 + \alpha Ce^{\beta}} \quad (4)$$

$$qe = \frac{k\ qm\ Ce^{ns}}{1 + ks\ Ce^{ns}} \quad (5)$$

where, *qe* stands for the concentration of adsorbed contaminant on the adsorbent in mg/g, *qm* is the maximum capacity for adsorption of monolayer coverage in mg/g, *kl* is the constant related to the binding site affinity in L/mg, and Ce for the equilibrium amount of contaminant in mg/L, *Kf* and *n* are reprehensively Freundlich constants, related with bonding energy $(mg/g)(L/mg)^{1/n}$ and adsorption intensity and related with heterogeneity. *Krp* and *α*, in the Redlich–Peterson model(R-P) (Eq. (4)), represent isotherm constants of units of L/g, *β* (l/mg) is the exponent reflecting the heterogeneity of the sorbent, and *ks* is the affinity constant in the Sips model (l/mg). The fitting of the isotherm model data of LEVOX onto porcelanite and $NanoSiO_2$/porcelanite is presented in Figure 17 and Figure 18, respectively. Using an Excel solver, the parameter values derived from the nonlinear model are presented in Table 1. For the adsorption of LEVOX using porcelanite and $NanoSiO_2$/porcelanite, the fitting degree of these models was assessed by comparing their correlation coefficient. The following sequence was observed: Langmuir = Sips > Freundlich > Redlich-Peterson and Langmuir > Freundlich> Redlich-Peterson > Sips for adsorption using porcelanite and $NanoSiO_2$/porcelanite, respectively. The Sips isotherm and Redlich-Peterson were used to evaluate the monolayer adsorption of LEVOX. Table 1 shows that the ns and β of the Sips model and Redlich-Peterson, respectively, were equal to about 1, which confirms the Langmuir model. Furthermore, for both porcelanite and $NanoSiO_2$/porcelanite, the square root error (SSE) value for the Langmuir models is less than that of the other models. These suggest that a monolayer and a homogenous system largely dominate the surface of both porcelanite and $NanoSiO_2$/porcelanite, and all the sites of the surface are equivalent and can adsorb one molecule. In addition to that, there is no interaction between sorbet molecules on adjacent sites. The maximum adsorption capacity was 52.322 and 130 mg/g for porcelanite and $NanoSiO_2$/porcelanite, respectively. This is an improvement in that the coating of porcelanite with Nano-SiO_2 gives good results by increasing the value of maximum adsorption capacity; therefore, it is favorable for the adsorption of LEVOX compared with other adsorbents reported in Table 2. The RL (dimensionless constant factor) represents an essential characteristic of the Langmuir model, which can be obtained by Eq. (6) [35-37].

$$RL = \frac{1}{1 + KlCe} \quad (6)$$

The magnitude of *RL* helps predict the possibility of the irreversible adsorption system if *RL*=0, linear if *RL*=1, unfavorable if RL is larger than 1, and favorable if *RL* is between 1 and 0. As shown in Table 1, the values of *RL* were 0.595 and 0.506 for porcelanite and $NanoSiO_2$/porcelanite, respectively, indicating the favorability of the adsorption of LEVOX onto porcelanite and $NanoSiO_2$/porcelanite, respectively.

In this study, both porcelanite and its Nano-silica modified form demonstrated considerable effectiveness in adsorbing levofloxacin from aqueous solutions. The unmodified porcelanite showed a moderate adsorption capacity of 52.43 mg/g, outperforming several commonly used adsorbents, as shown in Table 2. More notably, the $NanoSiO_2$/porcelanite composite exhibited a significantly enhanced adsorption capacity of 130 mg/g, ranking among the higher-performing adsorbents reported in recent literature. This improvement is likely due to the increased surface area and the introduction of additional active sites provided by the Nano-silica, which facilitate stronger interactions with levofloxacin molecules. These results suggest that natural porcelanite, especially when modified with Nano-sized silica, holds substantial potential as an effective and sustainable adsorbent for removing pharmaceutical contaminants such as levofloxacin from water [37].

Table 1. Parameter values of isotherm models for the adsorption of LEVOX onto porcelanite and $NanoSiO_2$/porcelanite

Model	Porcelanite (PC)	$NanoSiO_2$/Porcelanite
Langmuir	qmax 52.322	130
	Kl 0.0208	0.044
	RL 0.595	0.507
	SSE 0.2756	2.979
	R^2 0.998	0.997
Freundlich	Kf 1.294	8.013
	n 1.196	1.500
	SSE 0.683	19.43
	R^2 0.995	0.987
Redlich-Peterson	Krp 0.850	9.25
	α 0.002	0.1647
	β 0.998	0.999
	SSE 2.52	41.520
	R^2 0.989	0.973
Sips	qs 52	130
	Ks 0.02	0.04
	ns 1	1
	SSE 1.0708	4.249
	R^2 0.998	0.936

Table 2. Adsorption capacity of LEVOX by different adsorbents

Adsorbent	qm (mg/g)	References
Raw rice husk (RRH)	2.47	[38]
Alumina-doped coconut coir charcoal	1.15	[39]
Fe_3O_4@SiO_2	6.85	[40]
Magnesium-supported biochar	25.2	[41]
Powder zeolite (FAU-1)	31.32	[42]
Zeolite	35.5	[43]
Fe-P-Mt	48.61	[44]
Sunflower husk coated in CuO (CSFH)	62.24	[45]
MOFs, MIL-100 (Fe)	87.3	[46]
NBent-NTiO2-Chit	90.91	[47]
CaO/MgO	107	[48]
$MnFe_2O_3$/GO core-shell	133	[49]
Fe/Mn-BC	181	[50]
Porcelanite	52.43	Current study
$NanoSiO_2$/porcelanite	130	Current study

3.8 Kinetic study of LEVOX adsorption

To model the adsorbent-adsorbate interaction, the kinetic models comprise the pseudo-first-order, pseudosecond-order, intraparticle diffusion, and Elovich models, which are represented, respectively, in the following Eqs. (7)-(10).

These kinetic models utilised in the current investigation are represented by the following equations [5, 51].

$$q(t) = q_e\,(1 - e^{-K_1 t}) \quad (7)$$

$$q(t) = \frac{K_2\, {q_e}^2 t}{1 + K_2 q_e t} \quad (8)$$

$$q(t) = kid\; t^{0.5} + c \quad (9)$$

$$q(t) = \frac{1}{\beta} ln(1 + \alpha\, \beta t) \quad (10)$$

where, $q(t)$ denotes the amount of adsorbate adsorbed onto the adsorbent at any t time (mg/g), K_1 is constant represents the rate of the pseudo-first-order (min^{-1}), K_2 is a constant value that denotes the rate of the pseudo-second-order (g/mg. min), The symbol q_e signifies the amount of solute adsorbed onto the adsorbent at equilibrium (mg/g). *Kid* represents the rate constant for intraparticle diffusion (mg/g $min^{0.5}$). On the other hand, C represents the boundary layer thickness (mg/g) [49, 52, 53]. α and β stand for the initial adsorption rate constants and parameters associated with the activation energy during the adsorption process, respectively.

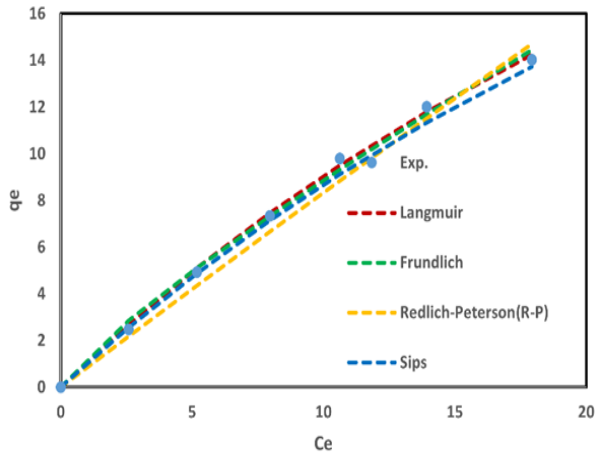

Figure 17. Isotherm models for the adsorption of LEVOX onto porcelanite

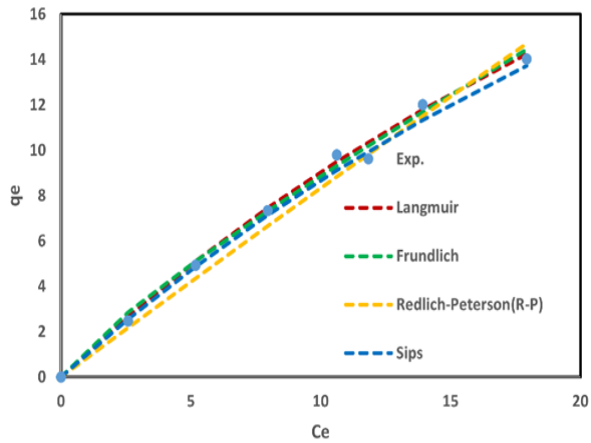

Figure 18. Isotherm models for the adsorption of LEVOX onto $NanoSiO_2$/porcelanite

Figures 19 and 20 show the plots of the Pseudo-first-order, pseudo-second-order, and Elovich models for the LEVOX removal onto porcelanite and $NanoSiO_2$/porcelanite, respectively. Parameters of kinetic models were determined using the Excel Solver. The extracted parameters of the kinetic models for removing LEVOX onto porcelanite and $NanoSiO_2$/porcelanite are shown in Table 3. Based on the correlation coefficients R^2 achieved for pseudo-second order adsorption of LEVOX onto porcelanite and $NanoSiO_2$/porcelanite, they are greater than pseudo-first order kinetics. Furthermore, the equilibrium capacity (q_e) attained from pseudo-second order kinetics is in par with the experimental value. Suggested that both the experimental data of adsorption of LEVOX onto porcelanite and $NanoSiO_2$/porcelanite are fitting with pseudo-second order kinetics. The applicability of the pseudo-second-order model shows that chemisorption dominates over physisorption. Consequently, the electron transfer or valence forces between LEVOX and the adsorbent surface are important in adsorption. Moreover, the Elovich model helps describe the heterogeneous surface. According to the value of R^2 (for the Elovich kinetic model) of 0.994 and 0.984 for porcelanite and $NanoSiO_2$/porcelanite, respectively, it is suggested that the Elovich model is convenient for evaluating the adsorption data, which confirms that both porcelanite and $NanoSiO_2$/porcelanite surfaces are energetically heterogeneous surfaces and that chemisorption interactions occur.

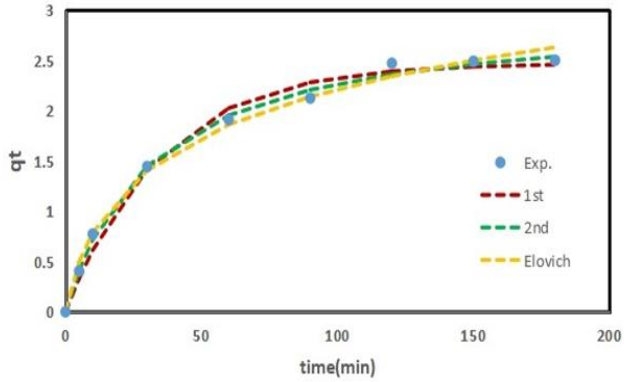

Figure 19. The Kinetic models for the adsorption of LEVOX onto porcelanite

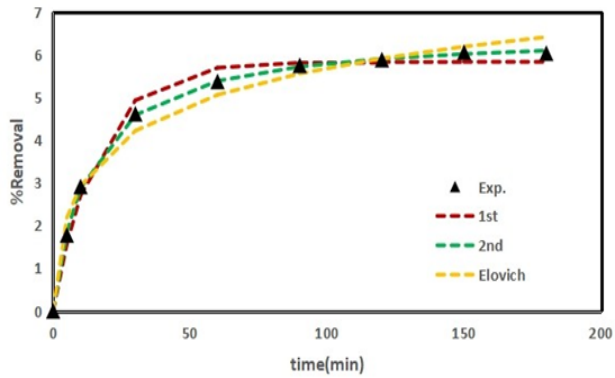

Figure 20. The Kinetic models for adsorption of LEVOX onto $NanoSiO_2$/porcelanite

Figures 21 and 22 state the intraparticle diffusion model by plotting the square root of time ($t^{0.5}$) against the equilibrium adsorption rate for removing LEVOX onto porcelanite and $NanoSiO_2$/porcelanite, respectively. These figures show that neither straight line passes through the origin point, indicating that intraparticle diffusion was involved and that other mechanisms contributed [54].

Table 3. Thermodynamic parameters of LEVOX adsorption onto porcelanite and NanoSiO$_2$/porcelanite

Model		Porcelanite	NanoSiO$_2$/Porcelanite
Pseudo-first order	qexp.	2.900	6.0306
	qe	2.473	5.525
	K1	0.028	0.06224
	SSE	0.080	0.39006
	R^2	0.991	0.990
Pseudo-second order	qe	2.983	6.077
	K2	0.010	0.0121
	SSE	0.258	0.0133
	R^2	0.999	0.9996
Intraparticle diffusion (Ipd)	KIpd	0.190	0.3583
	C	0.224	1.8977
	SSE	0.257	2.631
	R^2	0.966	1
Elovich	β	1.357	0.804
	α		1.848
	SSE	0.046	0.680
	R^2	0.994	0.984

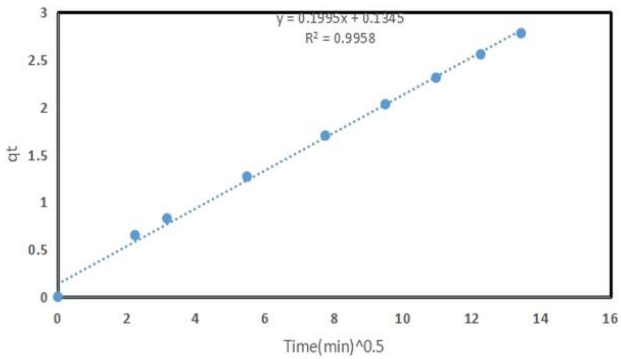

Figure 21. The Ipd for Kinetic models for adsorption of LEVOX onto porcelanite

3.9 Thermodynamic study for the adsorption of LEV

Briefly, to understand the behavior of LEVOX adsorption onto porcelanite, NanoSiO$_2$/porcelanite was investigated thermodynamically [36]. Eqs. (11)-(13) evaluate the thermodynamic parameters from the following equations: Gibbs free energy, ΔGO, enthalpy, ΔHo, and entropy, ΔSO.

$$\Delta GO = \Delta HO - T\,\Delta SO \quad (11)$$

$$\Delta GO = -RT\ln Kd \quad (12)$$

$$\mathrm{Lnkd}=\ln(qe/Ce)=(\Delta SO/R)-(\Delta HO/RT) \quad (13)$$

where, T (°K) denotes absolute temperature, *kd* (l/g) is a constant representing the adsorption equilibrium distribution, and *R* corresponds to the gas constant (8.314 J/mol.K). Table 4 shows the estimated Enthalpy [24]. Gibbs free energy change, and entropy for LEVO adsorption at temperatures of 25, 30, and 35°C. The negative ΔHo value denotes the exothermic nature of adsorption, and the adsorption of LEVOX onto porcelanite and NanoSiO$_2$/porcelanite is not favored at higher temperatures. The negative ΔGo values confirm the spontaneous adsorption of LEVOX at all tested temperatures. However, a decreasing ΔGo value (i.e., it becomes less harmful) and an increasing temperature reflect a lower feasibility of the sorption process. The negative ΔS° value indicates less randomness at the solid-solution interface. The value of ΔHo states that the Adsorption is physical if the ΔHo range is (5-40 KJ/mole) or chemical if the ΔHo range is (40-800 KJ/mole). The values of ΔHo onto porcelanite and NanoSiO$_2$/porcelanite from Table 4 indicated that the adsorption of LEVOX onto porcelanite and NanoSiO$_2$/porcelanite proposes chemisorption [38].

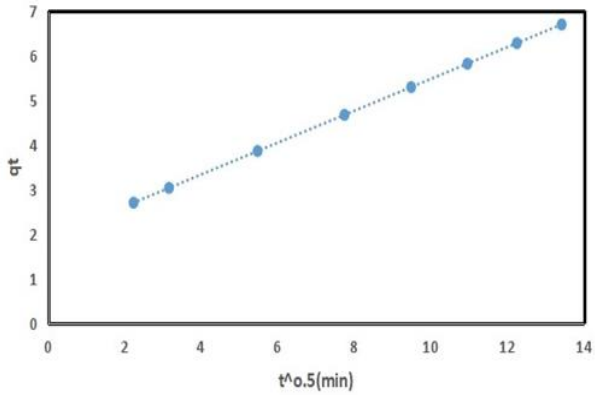

Figure 22. The Ipd for Kinetic models for adsorption of LEVOX onto NanoSiO$_2$/porcelanite

3.10 Reusability of adsorbent

The ability to regenerate porcelanite and NanoSiO$_2$/porcelanite is essential for evaluating its industrial application feasibility. The regeneration of porcelanite and NanoSiO$_2$/porcelanite was performed using 2M ethanol. Figure 23 shows that after six adsorption-desorption cycles, LEVOX removal is higher than 25% and 75% for porcelanite and NanoSiO$_2$/porcelanite, respectively, compared to the first cycle. This confirms the high stability of NanoSiO$_2$/porcelanite.

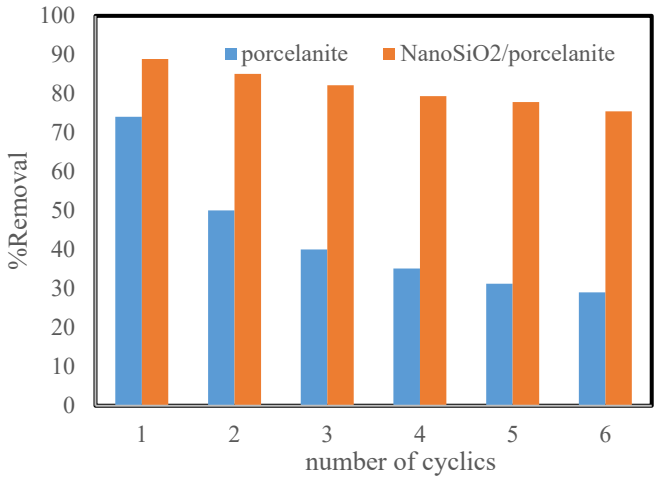

Figure 23. Reusability of porcelanite and NanoSiO$_2$/porcelanite for the removal of LEVOX

Table 4. Thermodynamic parameters of LEVOX adsorption onto porcelanite and $NanoSiO_2$/porcelanite

	Porcelanite				NanoSiO₂/Porcelanite			
Temp. (ºC)	ΔGo	ΔHo	ΔSo	R^2	ΔGo	ΔHo	ΔSo	R^2
25	-2.664				-4.876			
30	-2.027	-40.60	-0.13	0.997	-3.861	-65.34	-0.20	0.974
35	-0.117				-0.818			

4. CONCLUSIONS

This study showed that untreated Iraqi porcelanite and its modified version with silica nanoparticles ($NanoSiO_2$/porcelanite) are good at removing levofloxacin from water in batch adsorption tests. Several operational factors significantly influenced adsorption efficiency, including the pH, initial concentration of levofloxacin, adsorbent dosage, shaking speed, contact time, particle size, and temperature. Under optimized conditions at pH 6.5, 424 µm particle size, and a temperature of 298.15 K, the $NanoSiO_2$/porcelanite material showed notably enhanced performance, requiring only 0.08 g per 50 mL for effective removal compared to 0.15 g for raw porcelanite. The percent removal reached 91% on $NanoSiO_2$/porcelanite and 74% on porcelanite. The pseudo-second-order model and the kinetic data supported chemisorption as the main adsorption method. Moreover, equilibrium data, which show monolayer adsorption behaviour, best fit the Langmuir isotherm model. The highest amount of adsorption that the $NanoSiO_2$/porcelanite reached was 130 mg/g, significantly outperforming raw porcelanite, which showed a 52.322 mg/g capacity. These results confirm that silica nanoparticle modification improves the material's surface properties and adsorption potential.

Moreover, regeneration experiments using 2M ethanol demonstrated the adsorbents' stability over consecutive cycles. $NanoSiO_2$/porcelanite maintained over 75% (reduced only 13%) LEVOX removal efficiency after six cycles, compared to only 25% (reduced only 45%) for unmodified porcelanite, highlighting its durability and practical potential for long-term application. These findings indicate that silica modification not only enhances adsorption performance but also extends the material's operational lifespan, making it a strong candidate for practical application in water treatment systems. Nevertheless, the influence of real wastewater conditions remains to be explored. Future studies should focus on pilot-scale testing, evaluation under variable environmental conditions, and cost-benefit analysis to better assess the material's feasibility for large-scale implementation. Despite these limitations, the modified porcelanite offers a promising, low-cost, and regenerable solution for the efficient removal of LEVOX residues from contaminated water sources.

ACKNOWLEDGMENT

We are appreciative of the Department of the University of Baghdad's Environmental Engineering College of Engineering for helping with the lab work.

REFERENCES

[1] Altaf, M.A., Sharma, N., Singh, J., et al. (2023). Mechanistic insights on melatonin-mediated plant growth regulation and hormonal cross-talk process in solanaceous vegetables. Scientia Horticulturae, 308: 111570. https://doi.org/10.1016/j.scienta.2022.111570

[2] Shahbazi, A., Hamidian, A.H., Zhang, Y., Yang, M. (2025). Adsorption of fluoroquinolone antibiotics in aqueous solutions using nanomaterials: Mechanisms, challenges, and future perspectives. Nanotechnology for Environmental Engineering, 10: 25. https://doi.org/10.1007/s41204-025-00417-9

[3] Wang, H., Liu, Y., Wei, S., Yao, S., Zhang, J., Huang, H. (2016). Selective extraction and determination of fluoroquinolones in bovine milk samples with montmorillonite magnetic molecularly imprinted polymers and capillary electrophoresis. Analytical and Bioanalytical Chemistry, 408: 589-598. https://doi.org/10.1007/s00216-015-9140-1

[4] Liu, Y., Dong, C., Wei, H., Yuan, W., Li, K. (2015). Adsorption of levofloxacin onto an iron-pillared montmorillonite (clay mineral): Kinetics, equilibrium and mechanism. Applied Clay Science, 118: 301-307. https://doi.org/10.1016/j.clay.2015.10.010

[5] Alsaheb, Z.A., Hummadi, K.K. (2025). Synthesis, characterization, and evaluation of Nano MgO/bentonite composite for efficient AMOX adsorption from wastewater. International Journal of Design & Nature and Ecodynamics, 20(6): 1243-1255. https://doi.org/10.18280/ijdne.200606

[6] Bednárek, J., Matějová, L., Koutník, I., Vráblová, M., Juan Francisco Cruz, G., Strašák, T., Šiler, P., Hrbáč, J. (2024). Revelation of high-adsorption-performance activated carbon for removal of fluoroquinolone antibiotics from water. Biomass Conversion and Biorefinery, 14: 2585-2599. https://doi.org/10.1007/s13399-022-02577-z

[7] Atta, H.A., Hummadi, K.K., M-Ridha, M.J. (2022). The application of response surface methodology and Design-Expert® for analysis of ciprofloxacin removal from aqueous solution using raw rice husk: Kinetic and isotherm studies. Desalination and Water Treatment, 248: 203-216. https://doi.org/10.5004/dwt.2022.28074

[8] Yao, H., Lu, J., Wu, J., Lu, Z., Wilson, P.C., Shen, Y. (2013). Adsorption of fluoroquinolone antibiotics by wastewater sludge biochar: Role of the sludge source. Water, Air, & Soil Pollution, 224: 1370. https://doi.org/10.1007/s11270-012-1370-7

[9] Liu, T., Liu, W., Li, X., Wang, H., Lan, Y., Zhang, S., Wang, Y., Liu, H. (2024). Effect of environmental factors on adsorption of ciprofloxacin from wastewater by microwave alkali modified fly ash. Scientific Reports, 14(1): 19831. https://doi.org/10.1038/s41598-024-70921-6

[10] Van Wieren, E.M., Seymour, M.D., Peterson, J.W. (2012). Interaction of the fluoroquinolone antibiotic, ofloxacin, with titanium oxide nanoparticles in water:

Adsorption and breakdown. Science of the Total Environment, 441: 1-9. https://doi.org/10.1016/j.scitotenv.2012.09.067

[11] Bhogal, S., Mohiuddin, I., Kaur, K., Kim, K., Malik, A.K. (2023). Mesoporous silica imprinted nanocomposites for selective adsorption and detection of levofloxacin. Journal of Water Process Engineering, 57: 104693. https://doi.org/10.1016/j.jwpe.2023.104693

[12] Mohammad, M.R., Ahmed, D.S., Mohammed, M.K.A. (2019). Synthesis of Ag-doped TiO_2 nanoparticles coated with carbon nanotubes by the sol–gel method and their antibacterial activities. Journal of Sol-Gel Science and Technology, 90: 498-509. https://doi.org/10.1007/s10971-019-04973-w

[13] Sharifian, S., Asasian-Kolur, N., Najafi, H., Haddadi, B., Jordan, C., Harasek, M. (2023). Reusable granulated silica pillared clay for wastewater treatment, selective for adsorption of Ni (II). Cleaner Engineering and Technology, 14: 100634. https://doi.org/10.1016/j.clet.2023.100634

[14] da Silva de Assis, D.A., dos Santos, E.G., Eiras, D. (2024). Efficient and reusable mesoporous silica structures for ciprofloxacin removal from water media. Journal of Water Process Engineering, 60: 105144. https://doi.org/10.1016/j.jwpe.2024.105144

[15] Otalvaro, J.O., Avena, M., Brigante, M. (2019). Adsorption of norfloxacin on a hexagonal mesoporous silica: isotherms, kinetics and adsorbent reuse. Adsorption, 25: 1375-1385. https://doi.org/10.1007/s10450-019-00100-x

[16] Zeidman, A.B., Rodriguez-Narvaez, O.M., Moon, J., Bandala, E.R. (2020). Removal of antibiotics in aqueous phase using silica-based immobilized nanomaterials: A review. Environmental Technology & Innovation, 20: 101030. https://doi.org/10.1016/j.eti.2020.101030

[17] Hamad, M.T.M.H., El-Sesy, M.E. (2023). Adsorptive removal of levofloxacin and antibiotic resistance genes from hospital wastewater by nano-zero-valent iron and nano-copper using kinetic studies and response surface methodology. Bioresources and Bioprocessing, 10(1): 1-29. https://doi.org/10.1186/s40643-022-00616-1

[18] Sivolapov, P., Myronyuk, O., Baklan, D. (2022). Synthesis of Stober silica nanoparticles in solvent environments with different Hansen solubility parameters. Inorganic Chemistry Communications, 143: 109769. https://doi.org/10.1016/j.inoche.2022.109769

[19] Hasan, Y.R., Shaban, M.A.A., Ibrahim, M.A., Ridha, M.J., Hussein, H.A. (2023). Effect of calcination temperature on the adsorption performance of Mg/Al layered double hydroxide nanoparticles in the removal of meropenem antibiotics. The Iraqi Journal of Agricultural Science, 54(1): 42-58. https://doi.org/10.36103/ijas.v54i1.1675

[20] Zhang, B., Wang, Z., Huang, B., Zhang, X., Qin, X., Li, H., Dai, Y., Li, Y. (2016). Anisotropic photoelectrochemical (PEC) performances of ZnO single-crystalline photoanode: Effect of internal electrostatic fields on the separation of photogenerated charge carriers during PEC water splitting. Chemistry of Materials, 28(18): 6613-6620. https://doi.org/10.1021/acs.chemmater.6b02639

[21] Kumar, A.P., Bilehal, D., Tadesse, A., Kumar, D. (2021). Photocatalytic degradation of organic dyes: Pd-γ-Al_2O_3 and PdO-γ-Al_2O_3 as potential photocatalysts. RSC Advances, 11(11): 6396-6406. https://doi.org/10.1039/D0RA10290C

[22] Zhang, T., Su, H., Shi, X., Li, C. (2022). Self-healing siloxane elastomers constructed by hierarchical covalent crosslinked networks and reversible dynamic bonds for flexible electronics. Journal of Materials Science, 57(22): 10444-10456. https://doi.org/10.1007/s10853-022-07293-7

[23] Li, N., Lu, W., Zhu, D. (2023). Amino-functionalized silica@Resorcinol–formaldehyde nanocomposites for the removal of Cr(VI) from aqueous solutions. Polymers, 15(20): 4094. https://doi.org/10.3390/polym15204094

[24] Al-Jubouri, A.K., Al-Saadi, N.H., Kadhim, M.A. (2022). Green synthesis of copper nanoparticles from myrtus communis leaves extract characterizattion, antioxidant and catalytic activity. Iraqi Journal of Agricultural Sciences, 53(2): 471-486. https://doi.org/10.36103/ijas.v53i2.1555

[25] Mohammed, A.A., Kareem, S.L. (2021). Enhancement of ciprofloxacin antibiotic removal from aqueous solution using ZnO nanoparticles coated on pistachio shell. Desalination and Water Treatment, 213: 229-239. https://doi.org/10.5004/dwt.2021.26674

[26] Fadhel, M.H., Al Khazraji, A.H., Fahmi, A.H. (2023). Eco-Friendly Method for Synthesis of Mn_3O_4 Nanoparticles and Their Characterization. Egyptian Journal of Chemistry, 66(7): 113-117. https://doi.org/10.21608/ejchem.2022.142687.6249

[27] Joni, I.M., Nulhakim, L., Vanitha, M., Panatarani, C. (2018). Characteristics of crystalline silica (SiO_2) particles prepared by simple solution method using sodium silicate (Na_2SiO_3) precursor. Journal of Physics: Conference Series, 1080: 012006. https://doi.org/10.1088/1742-6596/1080/1/012006

[28] Dubey, R.S., Rajesh, Y.B.R.D., More, M.A. (2015). Synthesis and characterization of SiO_2 Nanoparticles via sol-gel method for industrial applications. Materials Today: Proceedings, 2(4-5): 3575-3579. https://doi.org/10.1016/j.matpr.2015.07.098

[29] Elizondo-Villarreal, N., Gandara-Martínez, E., García-Méndez, M., Gracia-Pinilla, M., Guzmán-Hernández, A.M., Castaño, V.M., Gómez-Rodríguez, C. (2024). Synthesis and Characterization of SiO_2 Nanoparticles for Application as Nanoadsorbent to Clean Wastewater. Coatings, 14(7): 919. https://doi.org/10.3390/coatings14070919

[30] Foo, K.Y., Hameed, B.H. (2010). Insights into the modeling of adsorption isotherm systems. Chemical Engineering Journal, 156(1): 2-10. https://doi.org/10.1016/j.cej.2009.09.013

[31] Ho, Y.S., McKay, G. (1999). Pseudo-second order model for sorption processes. Process Biochemistry, 34(5): 451-465. https://doi.org/10.1016/S0032-9592(98)00112-5

[32] Corda, N.C., Kini, M.S. (2018). A review on adsorption of cationic dyes using activated carbon. MATEC Web of Conferences, 144: 02022. https://doi.org/10.1051/matecconf/201814402022

[33] Weber, W.J., Morris, J.C. (1963). Kinetics of adsorption on carbon from solution. Journal of the Sanitary Engineering Division, 89(2): 31-60. https://doi.org/10.1061/JSEDAI.0000430

[34] Cruz-Cruz, A., Rivas-Sanchez, A., Gallareta-Olivares, G., González-González, R.B., Cárdenas-Alcaide, M.F., Iqbal, H.M., Parra-Saldívar, R. (2023). Carbon-based

materials: adsorptive removal of antibiotics from water. Water Emerging Contaminants & Nanoplastics, 2: 2. https://doi.org/10.20517/wecn.2022.19

[35] Hammari, A.M., Abubakar, H., Misau, M.I., Aroke, U.O., Hamza, U.D. (2020). Adsorption equilibrium and kinetic studies of methylene blue dye using groundnut Shell and sorghum husk biosorbent. Journal of Environmental Bioremediation and Toxicology, 3(2): 32-39. https://doi.org/10.54987/jebat.v3i2.556

[36] Hummadi, K.K., Luo, S., He, S. (2022). Adsorption of methylene blue dye from the aqueous solution via bio-adsorption in the inverse fluidized-bed adsorption column using the torrefied rice husk. Chemosphere, 287: 131907. https://doi.org/10.1016/j.chemosphere.2021.131907

[37] Hummadi, K.K., Zhu, L., He, S. (2023). Bio-adsorption of heavy metals from aqueous solution using the ZnO-modified date pits. Scientific Reports, 13(1): 22779. https://doi.org/10.1038/s41598-023-50278-y

[38] Atta, H.A., Hummadi, K.K., M-Ridha, M.J. (2023). A sustainable raw rice husk adsorbent for effective levofloxacin removal from aqueous solution: Kinetic, thermodynamic and isotherm studies. Iraqi Journal of Agricultural Sciences, 54(5): 1407-1420. https://doi.org/10.36103/ijas.v54i5.1841

[39] Limbikai, S.S., Deshpande, N.A., Kulkarni, R.M., Khan, A.A.P., Khan, A. (2016). Kinetics and adsorption studies on the removal of levofloxacin using coconut coir charcoal impregnated with Al_2O_3 nanoparticles. Desalination and Water Treatment, 57(50): 23918-23926. https://doi.org/10.1080/19443994.2016.1138330

[40] Al-Jabari, M.H., Sulaiman, S., Ali, S., Barakat, R., Mubarak, A., Khan, S.A. (2019). Adsorption study of levofloxacin on reusable magnetic nanoparticles: Kinetics and antibacterial activity. Journal of Molecular liquids, 291: 111249. https://doi.org/10.1016/j.molliq.2019.111249

[41] Zhao, X., Yi, S., Dong, S., Xu, H., Sun, Y., Hu, X. (2018). Removal of levofloxacin from aqueous solution by Magnesium-impregnated Biochar: Batch and column experiments. Chemical Speciation & Bioavailability, 30(1): 68-75. https://doi.org/10.1080/09542299.2018.1487775

[42] de Sousa, D.N.R., Insa, S., Mozeto, A.A., Petrovic, M., Chaves, T.F., Fadini, P.S. (2018). Equilibrium and kinetic studies of the adsorption of antibiotics from aqueous solutions onto powdered zeolites. Chemosphere, 205: 137-146. https://doi.org/10.1016/j.chemosphere.2018.04.085

[43] Motamedi, M., Mollahosseini, A., Negarestani, M. (2022). Ultrasonic-assisted batch operation for the adsorption of rifampin and reactive orange 5 onto engineered zeolite–polypyrrole/TiO_2 nanocomposite. International Journal of Environmental Science and Technology, 19(8): 7547-7564. https://doi.org/10.1007/s13762-022-03951-0

[44] Xiao, F., Wang, Y.Q., Xie, X.Y., et al. (2022). Preparation of Fe/C-Mt composite catalyst and ofloxacin removal by peroxymonosulfate activation. Separation and Purification Technology, 298: 121548. https://doi.org/10.1016/j.seppur.2022.121548

[45] Ibrahim, M.A., Shaban, M.A.A., Hasan, Y.R., et al. (2022). Simultaneous Adsorption of Ternary Antibiotics (Levofloxacin, Meropenem, and Tetracycline) by Sunflower husk coated with copper oxide nanoparticles. Journal of Ecological Engineering, 23(6): 30-42. https://doi.org/10.12911/22998993/147806

[46] Chaturvedi, G., Kaur, A., Umar, A., Khan, M.A., Algarni, H., Kansal, S.K. (2020). Removal of fluoroquinolone drug, levofloxacin, from aqueous phase over iron based MOFs, MIL-100 (Fe). Journal of Solid State Chemistry, 281: 121029. https://doi.org/10.1016/j.jssc.2019.121029

[47] Hamad, M.T.M.H., El-Sesy, M.E. (2023). Adsorptive removal of levofloxacin and antibiotic resistance genes from hospital wastewater by nano-zero-valent iron and nano-copper using kinetic studies and response surface methodology. Bioresources and Bioprocessing, 10(1): 1. https://doi.org/10.1186/s40643-022-00616-1

[48] AbuKhadra, M.R., Basyouny, M.G., AlHammadi, A.A., El-Sherbeeny, A.M., Salam, M.A. (2020). Enhanced decontamination of levofloxacin as toxic pharmaceutical residuals from water using CaO/MgO nanorods as a promising adsorbent. Scientific Reports, 10(1): 14828. https://doi.org/10.1038/s41598-020-71951-6

[49] Mpelane, S., Mketo, N., Mlambo, M., Bingwa, N., Nomngongo, P.N. (2022). One-step synthesis of a Mn-doped Fe_2O_3/GO core–shell nanocomposite and its application for the adsorption of levofloxacin in aqueous solution. ACS Omega, 7(27): 23302-23314. https://doi.org/10.1021/acsomega.2c01460

[50] Zhang, K., Huang, D., Zhang, Y., et al. (2023). Natural mineral-derived Fe/Mn-BC as efficient peroxydisulfate activator for 2, 4-dichlorophenol removal from wastewater: Performance and sustainable catalytic mechanism. Journal of Environmental Management, 335: 117540. https://doi.org/10.1016/j.jenvman.2023.117540

[51] Jumaah, A.M., Humadi, K.K. (2021). Catalytic cracking of furfural extract-40 over Ni/HY-zeolite catalyst. Journal of Engineering, 27(1): 66-78. https://doi.org/10.31026/j.eng.2021.01.05

[52] Raji, Z., Karim, A., Karam, A., Khalloufi, S. (2023). Adsorption of heavy metals: mechanisms, kinetics, and applications of various adsorbents in wastewater remediation—A review. Waste, 1(3): 775-805. https://doi.org/10.3390/waste1030046

[53] Najim, A.A., Ismail, Z.Z., Hummadi, K.K. (2022). Biodegradation potential of sodium dodecyl sulphate (SDS) by mixed cells in domestic and non-domestic actual wastewaters: Experimental and kinetic studies. Biochemical Engineering Journal, 180: 108374. https://doi.org/10.1016/j.bej.2022.108374

[54] Hummadi, K.K. (2021). Optimal operating conditions for adsorption of heavy metals from an aqueous solution by an agriculture waste. Iraqi Journal of Chemical and Petroleum Engineering, 22(2): 27-35. https://doi.org/10.31699/IJCPE.2021.2.4